Title: Aberrant interaction between FUS and SFPQ in neurons of a wide-range of FTLD spectrum diseases

Running head: The role of FUS-SFPQ in FTLD spectrum diseases

Shinsuke Ishigaki[1,2,4,#], Yuichi Riku[1,3], Yusuke Fujioka[1], Kuniyuki Endo[1], Nobuyuki Iwade[1], Kaori Kawai[1,2], Minaka Ishibashi[2], Satoshi Yokoi[1], Masahisa Katsuno[1], Hirohisa Watanabe[1,4,5], Keiko Mori[6], Akio Akagi[3], Osamu Yokota[7,8], Seishi Terada[7], Ito Kawakami[9,10], Naoki Suzuki[11], Hitoshi Warita[11], Masashi Aoki[11], Mari Yoshida[3], Gen Sobue[2,4,12,#]

[1]Department of Neurology, Nagoya University Graduate School of Medicine, Nagoya, Aichi, Japan

[2]Research Division of Dementia and Neurodegenerative Disease, Nagoya University Graduate School of Medicine, Nagoya, Aichi, Japan

[3]Department of Neuropathology, Institute for Medical Science of Aging, Aichi Medical University, Nagakute, Aichi, Japan

[4]Brain and Mind Research Center, Nagoya University, Nagoya, Aichi, Japan

[5]Department of Neurology, Fujita Health University, Toyoake, Aichi, Japan

[6]Department of Neurology, Oyamada Memorial Spa Hospital, Yokkaichi, Mie, Japan

[7]Department of Neuropsychiatry, Okayama University Graduate School of Medicine, Dentistry and Pharmaceutical Sciences, Okayama, Japan

[8]Department of Psychiatry, Kinoko Espoir Hospital, Kasaoka, Okayama, Japan

[9]Dementia Research project, Tokyo Metropolitan Institute of Medical Sciences, Setagaya, Tokyo, Japan

[10]Department of Psychiatry, Tokyo Metropolitan Matsuzawa Hospital, Setagaya, Tokyo, Japan

[11]Department of Neurology, Tohoku University Graduate School of Medicine, Sendai, Miyagi, Japan

[12]Aichi Medical University, Nagakute, Aichi, Japan

[#]Correspondence and requests for materials should be addressed to Shinsuke Ishigaki (ishigaki-ns@umin.net) or Gen Sobue (sobueg@med.nagoya-u.ac.jp).

Key Words: FTLD; FUS; SFPQ

Number of words: 2499

Number of figures: 3

Number of tables: 1

Number of supplementary figures: 6

Number of supplementary Tables: 2

Abstracts (197 Words <200)

Fused in sarcoma (FUS) is genetically and clinicopathologically linked to frontotemporal lobar degeneration (FTLD) and amyotrophic lateral sclerosis (ALS). We have previously reported that intranuclear interactions of FUS and Splicing factor, proline- and glutamine-rich (SFPQ) contribute to neuronal homeostasis. Disruption of the FUS-SFPQ interaction leads to an increase in the ratio of 4-repeat tau (4R-tau)/3-repeat tau (3R-tau), which manifests in FTLD-like phenotypes in mice. Here, we examined FUS-SFPQ interactions in 142 autopsied individuals with FUS-related ALS/FTLD (ALS/FTLD-FUS), TDP-43-related ALS/FTLD (ALS/FTLD-TDP), progressive supranuclear palsy (PSP), cortico-basal degeneration (CBD), Alzheimer disease (AD), or Pick disease (PiD) as well as controls. Immunofluorescent imaging showed impaired intranuclear colocalization of FUS and SFPQ in neurons of ALS/FTLD-FUS, ALS/FTLD-TDP, PSP, and CBD cases, but not in AD and PiD cases. Immunoprecipitation analyses of FUS and SFPQ revealed reduced interactions between the two proteins in ALS/FTLD-TDP and PSP cases, but not in those with AD. Furthermore, the ratio of 4R/3R-tau was elevated in cases with ALS/FTLD-TDP and PSP, but was largely unaffected in cases with AD. We concluded that impaired interactions between intranuclear FUS and SFPQ and the subsequent increase in the ratio of 4R/3R-tau constitute a common pathogenesis pathway in FTLD spectrum diseases.

Introduction

Fused in sarcoma (FUS), Transactive response (TAR) DNA-binding protein 43 (TDP-43), and tau are known pathologic proteins in the frontotemporal lobar degeneration (FTLD) spectrum, including FTLD, amyotrophic lateral sclerosis (ALS), progressive supranuclear palsy (PSP), and cortico-basal degeneration (CBD). TDP-43 and FUS are causative for ALS and FTLD, which collectively comprise a continuous disease spectrum of multisystem proteinopathies (Robberecht and Philips, 2013; Renton *et al.*, 2014; Riku *et al.*, 2014).

FUS and TDP-43 regulate multiple aspects of RNA metabolism, including alternative splicing. Mislocalization of FUS and TDP-43 from the nucleus to the cytoplasm results in aberrant cytoplasmic inclusions in the affected neurons of FUS- or TDP-43-related ALS and FTLD cases (Munoz *et al.*, 2009; Neumann *et al.*, 2009; Deng *et al.*, 2010; Mackenzie *et al.*, 2011a; Kobayashi *et al.*, 2013). 3-repeat (3R)-tau accumulates in Pick disease (PiD), whereas 4-repeat (4R)-tau predominant aggregations are associated with progressive supranuclear palsy (PSP) and cortico-basal degeneration (CBD) (Olney *et al.*, 2017).

Using a mouse model, we reported that FUS regulates alternative splicing of tau proteins in coordination with Splicing factor, proline- and glutamine-rich (SFPQ). Under normal conditions, the two proteins form a high-molecular-weight complex in the nucleus. Disease-associated mutations in FUS gene, however, disrupt formation of the complex resulting in unregulated alternative splicing of tau, a disproportional increase in the 4R-tau/3R-tau ratio, and eventually neurodegeneration (Ishigaki *et al.*, 2017).

Reductions in SFPQ have been shown to lead to neuronal loss in both the developmental and adult stages of mice (Takeuchi *et al.*, 2018). In addition, potential

SFPQ mutations occur in some familial ALS cases (Thomas-Jinu *et al.*, 2017), and loss of SFPQ from neuronal nuclei was observed in familial and sporadic ALS cases (Luisier *et al.*, 2018). Consequently, dysfunction of FUS and SFPQ in neuronal nuclei may be a common pathomechanism across FTLD, ALS, and other FTLD spectrum diseases.

This study assesses the intranuclear interaction between FUS and SFPQ in autopsied cases with FUS-, TDP-43-, or tau-related neurodegenerative disorders. In total, we evaluated 107 autopsied cases with FUS-related ALS or FTLD (ALS/FTLD-FUS), TDP-43-related ALS or FTLD (ALS/FTLD-TDP), PSP, CBD, Alzheimer disease (AD), and PiD, as well as 35 controls.

Methods

Cases

The clinical and pathological demographics of the cases are shown in Table 1. We performed immunohistochemical assays on samples collected from 14 cases with ALS/FTLD-FUS (7 cases with ALS-FUS; and 7 cases with FTLD-FUS), 24 cases with ALS/FTLD-TDP (9 cases with ALS-TDP; and 15 cases with FTLD-TDP), 25 cases with PSP, 8 cases with CBD, 31 cases with AD, and 5 cases with PiD. We also included age-matched controls that showed no signs of brain lesions (n = 35, average age at death: 70.5 ± 7.8). The causes of death included cancer (n = 11), infection (n = 8), auto-immune diseases (n = 4), and others (n = 12).

Frozen frontal cortex samples from 8 cases with ALS/FTLD-TDP, 5 cases with PSP, 5 cases with AD and 13 controls were biochemically assessed. Genetic assessment was available for five ALS/FTLD-FUS cases: two harbored the R521L mutation (Suzuki *et al.*, 2012), a third had an R521H mutation, and the remaining two had no *FUS*

mutations. Although the other cases exhibited sporadic onset, genetic profiling was not available.

Clinical examinations and autopsies were carried out at the Department of Neurology, Nagoya University Graduate School of Medicine, at the Department of Neuropathology, Institute for Medical Science of Aging, Aichi Medical University, and at the Department of Neurology, Tohoku University Graduate School of Medicine. Written informed consent was obtained from family members to archive tissues for pathological analyses. All human studies described in this report were approved by the appropriate Ethics Review Committees of Nagoya University Graduate School of Medicine, Tokyo Metropolitan Institute of Medical Sciences, Okayama University Graduate School of Medicine, Dentistry and Pharmaceutical Sciences, and Zikei Institute of Psychiatry. Each autopsy was performed within 9 h of post-mortem. Frontal lobe samples were snap frozen in liquid nitrogen and stored at -80°C for later biochemical analysis.

Clinicopathological analyses and disease-classification

Clinical review of the cases was retrospective. Gender, age of death, duration of symptomatic disease, subtype of dementia, family history, brain weight, and post-mortem delay were assessed. The included cases were classified into ALS/FTLD-FUS, ALS/FTLD-TDP, PSP, CBD, PiD, and AD groups. ALS was defined based on clinical criteria for ALS and the presence of neuronal inclusions in the lower motor neurons (Brooks *et al.*, 2000; Munoz *et al.*, 2009; Mackenzie *et al.*, 2011b; Riku *et al.*, 2014). FTLD was defined based on clinical manifestation of frontotemporal dementia (FTD) (Neary *et al.*, 1998) and the presence of neuronal inclusions in the frontotemporal lobes (Munoz *et al.*, 2009; Mackenzie *et al.*, 2011b; Riku *et al.*, 2014). PSP and CBD were

defined according to published clinical criteria for PSP (Hoglinger *et al.*, 2017) or cortico-basal syndrome (Armstrong *et al.*, 2013), respectively, and the presence of neuronal and glial 4R-tau aggregation (Yoshida, 2006). PiD was defined as having FTD symptoms (Neary *et al.*, 1998) and 3R-tau-immunopositive Pick bodies. AD cases were defined as having Alzheimer's type dementia (Dubois *et al.*, 2007) and demonstrated neurofibrillary tangle (NFT) of Braak stage IV or more and amyloid deposits of Thal phase 4 or more (Montine *et al.*, 2012).

Pathological analysis

The left hemisphere was fixed in 10% neutral-buffered formalin for at least one month. Frozen samples were collected from the right hemisphere. The fixed hemisphere was cut 5 mm posterior to the mammillary bodies, and 8-mm-thick coronal sections were systematically prepared. The tissues were embedded in paraffin and 4.5-μm-thick sections stained using hematoxylin-eosin (H-E) and Klüver-Barrera methods. The primary antibodies used are summarized in Supplementary Table 1. We compared the immunostaining of three anti-FUS and two anti-SFPQ antibodies and verified that their sensitivities and specificities were similar (Supplementary Fig. 1A).

Quantitative analysis of anti-SFPQ and anti-FUS immunofluorescence

Immunofluorescent imaging was done on a confocal laser microscopy (LSM710, Zeiss). We analyzed all sections under the same settings and acquired images from individual confocal planes. Fluorescent signals for FUS and SFPQ within the neuronal nucleus were obtained from the Betz cells of the primary motor cortex and hippocampal granule cells at 630x magnification. The Betz cells were identified in layer V of the

agranular, primary motor cortex (Brodmann area 4) based on their larger size relative to other pyramidal neurons (Paxinos, 1990). The hippocampal granule cells were anatomically identified as those surrounding the CA4. The neurons were immunohistochemically confirmed using anti-NeuN immunohistochemistry (Supplementary Fig. 1B). We randomly chose 12 nuclei for each patient; however, neurons with FUS-positive inclusions in ALS/FTLD-FUS cases were excluded. Second, the signal intensities (at 488 and 546 nm) from each intranuclear matrix that was along with the diameter of nuclei were automatically measured. Nuclei with diameters < 5 μm were excluded. The signals were acquired using ZEN 2012 software blue edition (Zeiss) as described (Matsuda *et al.*, 2002). Samples with average FUS or SFPQ signal intensities < 10 fluorescent-units were excluded. An R^2 value correlating the fluorescent intensities of FUS and SFPQ was calculated for the intranuclear matrixes along the diameter. An averaged R^2 value from the 12 neurons was defined as a case-specific mean value for FUS-SFPQ colocalization (Supplementary Fig. 1C).

Biochemical analysis

The immunoprecipitation and qPCR methods were described previously (Ishigaki *et al.*, 2017). Sequence data for both primers and an internal probe are listed in Supplementary Table 2.

Statistics

The clinical and pathological findings were compared using the Kruskal-Wallis method to assess bivariate correlations. The significance level was set at a p-value of 0.05 with the Bonferroni/Dunn correction applied for comparisons among multiple

groups. In the biochemical experiments, the differences were assessed with a paired t-test. The correlation index (R^2) and its significance level (p-value) were calculated with Pearson's regression. All the statistical tests were two-sided and were conducted using JMP14 (SAS Institute).

Data availability

The data that support the findings of this study are available from the corresponding author, upon reasonable request.

Results

Intranuclear colocalization of FUS and SFPQ

For the AD and control samples, immunofluorescent signals corresponding to SFPQ and FUS colocalized in the intranuclear matrix of hippocampal granule cells. In contrast, those signals were dissociated in the ALS/FTLD-FUS, ALS/FTLD-TDP, PSP, and CBD cases. Histopathologic findings from representative cases are shown (Fig. 1A, Supplementary Fig. 2). The correlation coefficient values (R^2), determined based on the fluorescent intensities of FUS and SFPQ in each intranuclear matrix, were reduced in the ALS/FTLD-FUS, ALS/FTLD-TDP, PSP, and CBD cases relative to controls, but were unchanged in the AD and PiD cases (Fig. 1B). These trends were similarly observed in the Betz cells of the primary motor cortex (Fig. 1, Supplementary Fig. 2).

The R^2 values for the intranuclear colocalization of FUS and SFPQ were calculated in the hippocampal granule cells of all cases (Fig. 2). The values were significantly lower in the ALS/FTLD-FUS (0.21 ± 0.03), ALS/FTLD-TDP (0.24 ± 0.03), PSP (0.21 ± 0.02), and CBD (0.21 ± 0.01) relative to controls (0.38 ± 0.02), but those with AD (0.41 ±

0.02) or PiD (0.50 ± 0.05) were unchanged (Table1, Kruskal-Wallis test with Bonferroni/Dunn correction for seven groups comparisons). The R^2 values did not differ between neurons with and without FUS-immunopositive inclusions in the ALS/FTLD-FUS cases (Supplementary Fig.3). There were also no significant differences between neurons with and without phosphorylated TDP-43 inclusions in the ALS/FTLD-TDP cases or between those with and without tau inclusions in the PSP or CBD cases (Supplementary Fig. 4).

Immunoprecipitation of SFPQ with FUS and qPCR of *MAPT* mRNA

Frozen frontal cortices were available for the ALS/FTLD-TDP, PSP, AD, and controls. Immunoprecipitation of SFPQ with an anti-FUS antibody was reduced in the ALS/FTLD-TDP and PSP cases relative to controls (Fig. 3A and B, and Supplementary Fig. 5A), while no significant differences were observed between AD cases and controls (Fig. 3C). The converse immunoprecipitation pairing yielded similar results (Fig. 3D). Because the FUS-SFPQ complex regulates the ratio of exon 10+/exon 10- via alternative splicing of *MAPT* (Ishigaki et al., 2017), we used qPCR to assess the exon 10+/exon 10- ratio of *MAPT* mRNA in the frontal cortices. We observed elevated ratios in the cases with ALS/FTLD-TDP and PSP relative to controls, indicating an increase in the 4-repeat (4R)-tau/3-repeat (3R)-tau ratio in *MAPT* mRNA splicing (Fig. 3E and F). In contrast, no significant differences were observed between the AD cases and controls (Fig. 3G). Immunoblotting analysis revealed a significant increase in the 4R-tau/3R-tau ratio in the cases with PSP but not in those with ALS/FTLD-TDP or AD (Supplementary Fig. 5B-D).

Varied expression of FUS and SFPQ in the nuclei of hippocampal granule cells

The fluorescent signal intensities of FUS and SFPQ were equivalent in the neuronal nuclei of the controls and AD cases. In contrast, the signal intensities were often disproportional in the ALS/FTLD-FUS, ALS/FTLD-TDP, PSP, and CBD cases with the fluorescent intensity of either SFPQ or FUS skewed higher than the other (Supplementary Fig. 6A and B). The expression variability, defined as the correlation between the SFPQ and FUS fluorescent intensities in approximately 400 nuclei for each patient, was significantly lower in cases with the ALS/FTLD-TDP and PSP than controls or AD cases (Supplementary Fig. 6C) (Table1, Kruskal-Wallis test with Bonferroni/Dunn correction for seven groups comparisons). The disproportionate intensities of SFPQ and FUS expression correlated positively with spatial dissociation of the proteins in the neuronal nuclei ($p < 0.001$) (Supplementary Fig. 6D).

Discussion

This study revealed spatial dissociation of SFPQ and FUS in the neuronal nuclei of ALS/FTLD-FUS, ALS/FTLD-TDP, PSP, and CBD. Immunohistochemical imaging showed clear dissociation in hippocampal granule cells and Betz cells with statistically supported quantitative analysis of the hippocampal granule cells. Immunoprecipitation studies showed limited FUS-based SFPQ precipitation in the cases with ALS/FTLD and PSP. In contrast, the intranuclear colocalization of FUS and SFPQ was retained in the AD cases. Our results indicate that interactions between FUS and SFPQ are impaired in the neuronal nuclei of FTLD-spectrum disorders associated with FUS, TDP-43, and 4R-tau, but not in AD. Impaired intranuclear interaction was similarly evident when neurons with and without FUS-, TDP-43-, or tau-aggregations were compared in the ALS/FTLD-FUS, ALS/FTLD-TDP, PSP, and CBD cases. Impaired interactions between FUS and SFPQ thus constitute a common pathogenic mechanism other than protein aggregation. It is, however, unclear if this pathway plays any role in the formation of neuronal inclusions.

Pathological and experimental data suggest common mechanisms contribute to neurodegenerative disorders with FUS, TDP-43, and 4R-tau aggregation. Cytoplasmic FUS aggregates are present in the motor neurons and iPSC-derived motor neurons of sporadic ALS-TDP cases (Deng *et al.*, 2010; Fujimori *et al.*, 2018; Ikenaka *et al.*, 2020). Widespread mislocalization of FUS in ALS motor neurons in the absence of aggregation suggests that loss of FUS function contributes to ALS (Tyzack *et al.*, 2019). Furthermore, risk factor genes overlap in sporadic ALS, sporadic FTLD, and PSP, support a common underlying pathogenic process (Karch *et al.*, 2018). 4R-tau pathologies were observed in a patient with FUS-positive basophilic inclusion body

disease (Wharton *et al.*, 2019) and a family carrying a Q140H substitution in *FUS* (Ferrer *et al.*, 2015).

Our study also demonstrated an increase in 4R-tau/3R-tau mRNA ratios in ALS/FTLD-TDP and PSP, but not in AD. Previously, we reported that suppression of FUS or SFPQ caused dysregulation of *MAPT* alternative splicing and subsequent predominance of the 4R-tau isoform in mice (Ishigaki *et al.*, 2017). These alterations in *MAPT* mRNA splicing appear to yield a 4R-tau-dominant condition in the neuronal nuclei of ALS/FTLD-TDP and PSP. However, because ALS/FTLD-TDP usually exhibit little to no 4R-tau aggregation, it remains unclear if the 4R-tau-dominant condition contributes to neuronal damage.

The intranuclear fluorescent intensities of SFPQ and FUS tended to be disproportional in the hippocampal granule cells of the ALS/FTLD-TDP, ALS/FTLD-FUS, and PSP cases. An index of the disproportion correlated positively with an index of FUS and SFPQ dissociation. While it is uncertain if the disproportional expression of FUS and SFPQ contributes to their spatial dissociation, the interactions between FUS and SFPQ may be necessary for their stability and persistence within the nucleus.

Although astrocytes and oligodendrocytes are also vulnerable to FTLD-spectrum diseases, the scope of FUS-SFPQ interactions in glial cells was unclear as the respective fluorescent signals were too weak to accurately examine colocalization levels (data not shown). Consequently, more sensitive immunochemical innovations optimized for glial cells are needed.

In conclusion, this study provides evidence for impaired intranuclear FUS-SFPQ interactions in FTLD-spectrum diseases associated with FUS, TDP-43, and 4R-tau, but

not in AD or PiD. The results suggest a specific and common pathogenic process across FTLD spectrum diseases other than neuronal inclusions.

Funding

This work was supported in part by JSPS KAKENHI; 26117004 (S.I.) and 15K09310 (S.I.), and JST; JPMJCR14G (S.I.). This research was also supported by the Japan Agency for Medical Research and Development (AMED); JP20dm0107059 (G.S.), JP19ek0109284 (G.S.), JP20ak0101111 (G.S.), JP20dm0207075 (S.I.), JP18dm0107105 (M.Y.), and JP16kk0205009 (M.Y.). Additional Support was provided by Grants-in Aid from the Research Committee of CNS Degenerative Diseases, Research on Policy Planning and Evaluation for Rare and Intractable Diseases, Health, Labour and Welfare Sciences Research Grants, the Ministry of Health, Labour and Welfare, Japan (M.Y.).

Competing interests

The authors report no competing interests.

Supplementary material

Supplementary material is available at Brain online.

References

Armstrong MJ, Litvan I, Lang AE, Bak TH, Bhatia KP, Borroni B*, et al.* Criteria for the diagnosis of corticobasal degeneration. Neurology 2013; 80: 496-503.

Brooks BR, Miller RG, Swash M, Munsat TL, World Federation of Neurology Research Group on Motor Neuron D. El Escorial revisited: revised criteria for the diagnosis of amyotrophic lateral sclerosis. Amyotroph Lateral Scler Other Motor Neuron Disord 2000; 1: 293-9.

Deng HX, Zhai H, Bigio EH, Yan J, Fecto F, Ajroud K*, et al.* FUS-immunoreactive inclusions are a common feature in sporadic and non-SOD1 familial amyotrophic lateral sclerosis. Ann Neurol 2010; 67: 739-48.

Dubois B, Feldman HH, Jacova C, Dekosky ST, Barberger-Gateau P, Cummings J*, et al.* Research criteria for the diagnosis of Alzheimer's disease: revising the NINCDS-ADRDA criteria. Lancet Neurol 2007; 6: 734-46.

Ferrer I, Legati A, Garcia-Monco JC, Gomez-Beldarrain M, Carmona M, Blanco R*, et al.* Familial behavioral variant frontotemporal dementia associated with astrocyte-predominant tauopathy. J Neuropathol Exp Neurol 2015; 74: 370-9.

Fujimori K, Ishikawa M, Otomo A, Atsuta N, Nakamura R, Akiyama T*, et al.* Modeling sporadic ALS in iPSC-derived motor neurons identifies a potential therapeutic agent. Nat Med 2018; 24: 1579-89.

Hoglinger GU, Respondek G, Stamelou M, Kurz C, Josephs KA, Lang AE*, et al.* Clinical diagnosis of progressive supranuclear palsy: The movement disorder society criteria. Mov Disord 2017; 32: 853-64.

Ikenaka K, Ishigaki S, Iguchi Y, Kawai K, Fujioka Y, Yokoi S*, et al.* Characteristic Features of FUS Inclusions in Spinal Motor Neurons of Sporadic Amyotrophic Lateral Sclerosis. J Neuropathol Exp Neurol 2020; 79: 370-7.

Ishigaki S, Fujioka Y, Okada Y, Riku Y, Udagawa T, Honda D*, et al.* Altered Tau Isoform Ratio Caused by Loss of FUS and SFPQ Function Leads to FTLD-like Phenotypes. Cell Rep 2017; 18: 1118-31.

Karch CM, Wen N, Fan CC, Yokoyama JS, Kouri N, Ross OA*, et al.* Selective Genetic Overlap Between Amyotrophic Lateral Sclerosis and Diseases of the Frontotemporal Dementia Spectrum. JAMA Neurol 2018; 75: 860-75.

Kobayashi Z, Kawakami I, Arai T, Yokota O, Tsuchiya K, Kondo H*, et al.* Pathological features of FTLD-FUS in a Japanese population: analyses of nine cases. J Neurol Sci 2013; 335: 89-95.

Luisier R, Tyzack GE, Hall CE, Mitchell JS, Devine H, Taha DM*, et al.* Intron retention and nuclear loss of SFPQ are molecular hallmarks of ALS. Nat Commun 2018; 9: 2010.

Mackenzie IR, Ansorge O, Strong M, Bilbao J, Zinman L, Ang LC*, et al.* Pathological heterogeneity in amyotrophic lateral sclerosis with FUS mutations: two distinct patterns correlating with disease severity and mutation. Acta Neuropathol 2011a; 122: 87-98.

Mackenzie IR, Neumann M, Baborie A, Sampathu DM, Du Plessis D, Jaros E*, et al.* A harmonized classification system for FTLD-TDP pathology. Acta Neuropathol 2011b; 122: 111-3.

Matsuda K, Ochiai I, Nishi M, Kawata M. Colocalization and ligand-dependent discrete distribution of the estrogen receptor (ER)alpha and ERbeta. Mol Endocrinol 2002; 16: 2215-30.

Montine TJ, Phelps CH, Beach TG, Bigio EH, Cairns NJ, Dickson DW*, et al.* National Institute on Aging-Alzheimer's Association guidelines for the neuropathologic assessment of Alzheimer's disease: a practical approach. Acta Neuropathol 2012; 123: 1-11.

Munoz DG, Neumann M, Kusaka H, Yokota O, Ishihara K, Terada S*, et al.* FUS pathology in basophilic inclusion body disease. Acta Neuropathol 2009; 118: 617-27.

Neary D, Snowden JS, Gustafson L, Passant U, Stuss D, Black S*, et al.* Frontotemporal lobar degeneration: a consensus on clinical diagnostic criteria. Neurology 1998; 51: 1546-54.

Neumann M, Rademakers R, Roeber S, Baker M, Kretzschmar HA, Mackenzie IR. A new subtype of frontotemporal lobar degeneration with FUS pathology. Brain 2009; 132: 2922-31.

Olney NT, Spina S, Miller BL. Frontotemporal Dementia. Neurol Clin 2017; 35: 339-74.

Paxinos G. The Human nervous system. San Diego: Academic Press; 1990.

Renton AE, Chio A, Traynor BJ. State of play in amyotrophic lateral sclerosis genetics. Nat Neurosci 2014; 17: 17-23.

Riku Y, Watanabe H, Yoshida M, Tatsumi S, Mimuro M, Iwasaki Y*, et al.* Lower motor neuron involvement in TAR DNA-binding protein of 43 kDa-related frontotemporal lobar degeneration and amyotrophic lateral sclerosis. JAMA Neurol 2014; 71: 172-9.

Robberecht W, Philips T. The changing scene of amyotrophic lateral sclerosis. Nat Rev Neurosci 2013; 14: 248-64.

Suzuki N, Kato S, Kato M, Warita H, Mizuno H, Kato M*, et al.* FUS/TLS-immunoreactive neuronal and glial cell inclusions increase with disease duration in familial amyotrophic lateral sclerosis with an R521C FUS/TLS mutation. J Neuropathol Exp Neurol 2012; 71: 779-88.

Takeuchi A, Iida K, Tsubota T, Hosokawa M, Denawa M, Brown JB*, et al.* Loss of Sfpq Causes Long-Gene Transcriptopathy in the Brain. Cell Rep 2018; 23: 1326-41.

Thomas-Jinu S, Gordon PM, Fielding T, Taylor R, Smith BN, Snowden V*, et al.* Non-nuclear Pool of Splicing Factor SFPQ Regulates Axonal Transcripts Required for Normal Motor Development. Neuron 2017; 94: 322-36 e5.

Tyzack GE, Luisier R, Taha DM, Neeves J, Modic M, Mitchell JS*, et al.* Widespread FUS mislocalization is a molecular hallmark of amyotrophic lateral sclerosis. Brain 2019; 142: 2572-80.

Wharton SB, Verber NS, Wagner BE, Highley JR, Fillingham DJ, Waller R*, et al.* Combined fused in sarcoma-positive (FUS+) basophilic inclusion body disease and atypical tauopathy presenting with an amyotrophic lateral sclerosis/motor neurone disease (ALS/MND)-plus phenotype. Neuropathol Appl Neurobiol 2019; 45: 586-96.

Yoshida M. Cellular tau pathology and immunohistochemical study of tau isoforms in sporadic tauopathies. Neuropathology 2006; 26: 457-70.

Figure Legends

Figure 1: Immunofluorescent imaging of intranuclear FUS and SFPQ

(A) The left panels show the hippocampal granule cells from representative cases. The sections were immunostained with anti-FUS and anti-SFPQ antibodies combined with DAPI-based (blue) nuclear staining. The FUS (red) and SFPQ (green) signals were colocalized within the intranuclear matrixes in the control sample. In contrast, the signals were dissociated within the nuclei of the FTLD-FUS, ALS-TDP, PSP, and CBD cases. The Betz cells from the same cases are shown in the right panels. Signals for FUS and SFPQ in Betz cell nuclei were also dissociated in FTLD-FUS, ALS-TDP, PSP, and CBD cases. Scale bars = 5 μm for left, 10 μm for right panels. (B) Raw quantitative colocalization indices for FUS and SFPQ from representative individual cases. The colocalization indices (R^2) for cases with ALS/FTLD-FUS (ALS/FTLD-FUS#1 and #2), ALS/FTLD-TDP (ALS/FTLD-TDP#1), PSP (PSP#1 and #2), and CBD (CBD#1 and #2) were lower than in cases with PiD (PiD#1), AD (AD#1 and #2), or the controls (Cont#1 and #2). Data shown are mean ± SEM.

Figure 2: Quantification of FUS and SFPQ intranuclear colocalization across disease groups

The colocalization indices in the hippocampal granule cells were calculated for all included cases and are displayed with mean ± SEM. The colocalization indices in the hippocampal granule cells were calculated for each disease group. The average colocalization indices were significantly lower in the ALS/FTLD-FUS, ALS/FTLD-TDP, PSP, and CBD cases than in the controls. No significant differences in the R^2 value were observed between the AD cases and the controls, or between the PiD cases and the

controls. Statistical analysis was performed using a Kruskal-Wallis test with significance levels set at $p < 0.05$ after Bonferroni/Dunn correction of the raw p-values for 7 group comparisons: the control (n = 28) vs. ALS/FTLD-FUS (n = 14), ALS/FTLD-TDP (n = 24), PSP (n = 25), CBD (n = 8), PiD (n = 5), or AD (n = 26).

Figure 3: Interactions between FUS and SFPQ are disrupted in the brain tissue of ALS/FTLD and PSP cases.

Frozen tissues of frontal cortex (prefrontal area) were available for cases with ALS/FTLD-TDP (n = 8), PSP (n = 5), or AD (n = 5), and controls (n = 13). The detailed methods were described in Supplemental material (Supplemental Fig. 5). (A) Protein extracts from the frontal lobe of ALS/FTLD-TDP cases and controls were immunoprecipitated with an anti-FUS antibody (A300-293A) and blotted with anti-SFPQ and anti-FUS antibodies (4H11). Immunoblots of the protein extracts (input) using anti-SFPQ, anti-FUS, and anti-α-Tubulin antibodies are also shown. The signal intensities for SFPQ in the FUS-immunoprecipitants were lower in ALS/FTLD-TDP cases than in controls (right graph, n = 8 for each, student t- test). (B) Immunoprecipitation of PSP cases also revealed lower FUS and SFPQ interactions than controls (n = 5 for each, student t- test). (C) FUS-SFPQ interactions were not disrupted in AD cases (n = 5 for each, student t- test). (D) The converse immunoprecipitation was performed for validation. Protein extracts from ALS/FTLD, PSP, and AD cases as well as controls were immunoprecipitated with an anti-SFPQ antibody (Bethyl Laboratories) and blotted with anti-SFPQ (abcam) and anti-FUS antibodies (4H11). Immunoblots of the protein extracts (input) using anti-SFPQ, anti-FUS, and anti-α-Tubulin antibodies are also shown. The results revealed lower FUS and SFPQ interactions than controls in

ALS/FTLD and PSP, but not in AD. (E) RNA was simultaneously extracted from samples shown in Fig. 3A from the frontal lobe of ALS/FTLD-TDP cases and controls. Subsequent qPCR analysis revealed that the splicing ratio of *MAPT* exon 10+/exon 10- (Ex10/Ex10-) was increased in ALS/FTLD-TDP cases relative to controls (n = 8 for each, student t-test). (F) The qPCR analysis revealed that the splicing ratio of *MAPT* exon 10+/exon 10- was increased in PSP cases relative to controls (n = 5 for each, student t-test). (G) In contrast, the splicing ratio of *MAPT* exon 10+/exon 10- was not elevated in AD cases (F) (n = 5 for each, student t-test). Data shown are mean ± SEM. Uncropped blots are available as Supplementary material.

Table.1 Clinical and pathological data

Pathological phenotypes	ALS/FTLD-FUS	ALS/FTLD-TDP	PSP	CBD	PiD	AD	controls	*p* Value
N (female/male)	14 (3/11)	24 (12/12)	25 (8/17)	8 (4/4)	5 (4/1)	31 (15/16)	35 (10/25)	
Age at death (year, SEM)	60.0 (3.9)	69.7 (1.7)	75.5 (1.2)	70.3 (1.6)	75.2 (4.4)	79.5 (1.6)	70.5 (1.3)	= 0.001*
Average Braak NFT stage (SEM)	0.58 (0.23)	1.09 (0.20)	1.80 (0.19)	-	-	5.05 (0.17)	1.33 (0.16)	< 0.001*
Average Thal Amyloid phase (SEM)	0.75 (0.43)	0.36 (0.14)	0.70 (0.24)	1.0 (0.82)	0.0 (0.0)	4.40 (0.13)	0.82 (0.20)	< 0.001*
N Used for IHC (female/male)	15 (3/12)	24 (12/12)	25 (8/17)	8 (4/4)	5 (4/1)	26 (13/13)	28 (7/21)	
FUS-SFPQ colocalization index (SEM)	0.21 (0.03)	0.24 (0.03)	0.21 (0.02)	0.21 (0.01)	0.50 (0.05)	0.41 (0.02)	0.38 (0.02)	= 0.004[#] = 0.004[##] < 0.001[†] = 0.040[††]
FUS-SFPQ expression variability index (SEM)	0.05 (0.01)	0.04 (0.01)	0.07 (0.02)	0.07 (0.03)	013 (0.05)	0.14 (0.02)	0.20 (0.03)	= 0.038[#] < 0.001[##] < 0.003[†]
N Used for IP and WB (female/male)	0	8 (3/5)	5 (2/3)	0	0	5 (2/3)	13 (6/7)	

ALS, amyotrophic lateral sclerosis; FTLD, frontotemporal lobar degeneration; PSP, progressive supranuclear palsy; CBD, cortico-basal degeneration; PiD, Pick's disease; AD, Alzheimer's disease
*AD versus controls, #ALS/FTLD-TDP versus controls, ##ALS/FTLD-TDP versus controls, †PSP versus controls, ††CBD versus controls.
Kruskal-Wallis test, significance level was determined by Bonferroni/Dunn correction for seven groups.

Figure 1

A

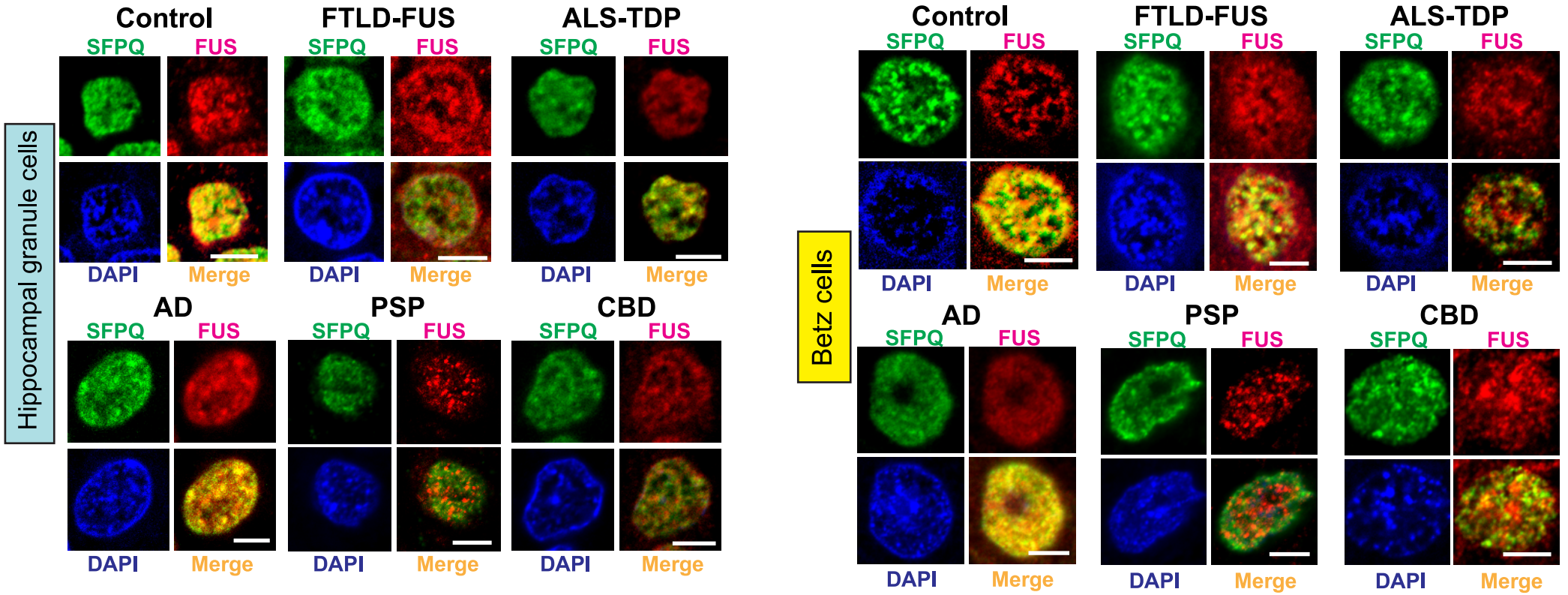
Control
FTLD-FUS
ALS-TDP
AD
PSP
CBD
SFPQ
FUS
DAPI
Merge
Hippocampal granule cells
Betz cells

B

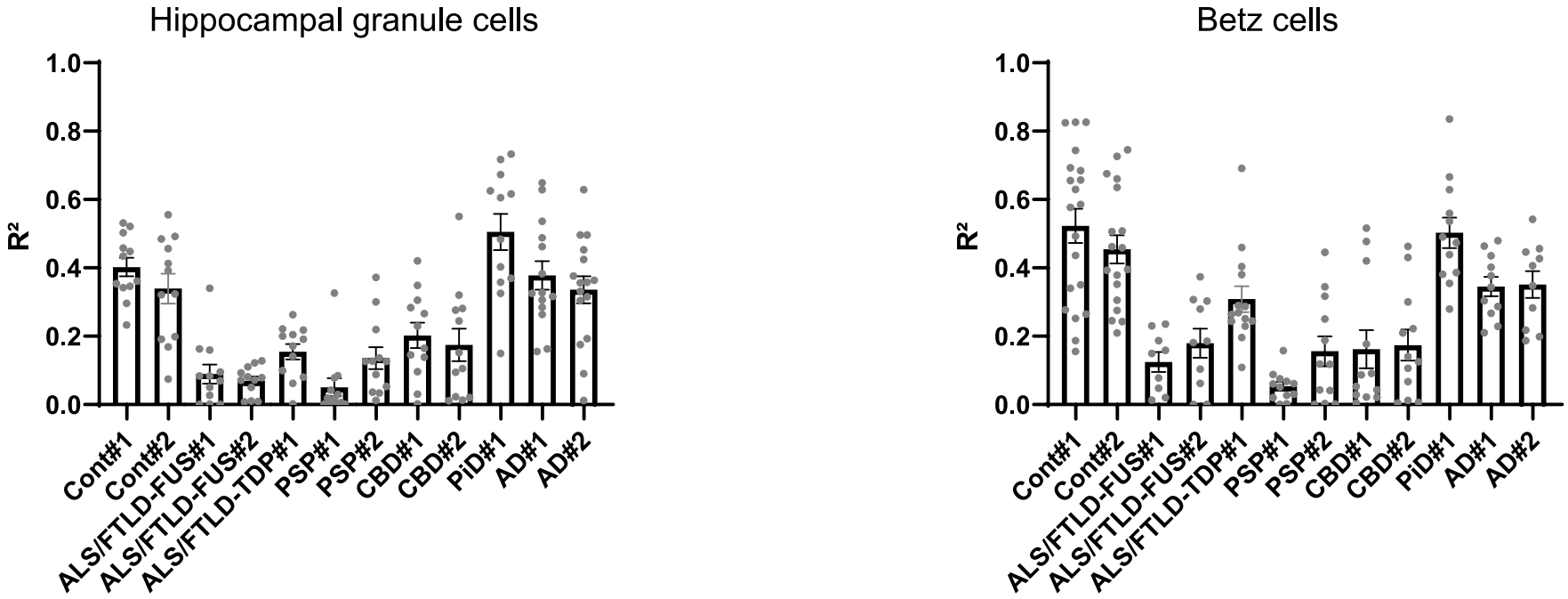
Hippocampal granule cells
Betz cells
R²
1.0
0.8
0.6
0.4
0.2
0.0
Cont#1
Cont#2
ALS/FTLD-FUS#1
ALS/FTLD-FUS#2
ALS/FTLD-TDP#1
PSP#1
PSP#2
CBD#1
CBD#2
PiD#1
AD#1
AD#2

Figure 2

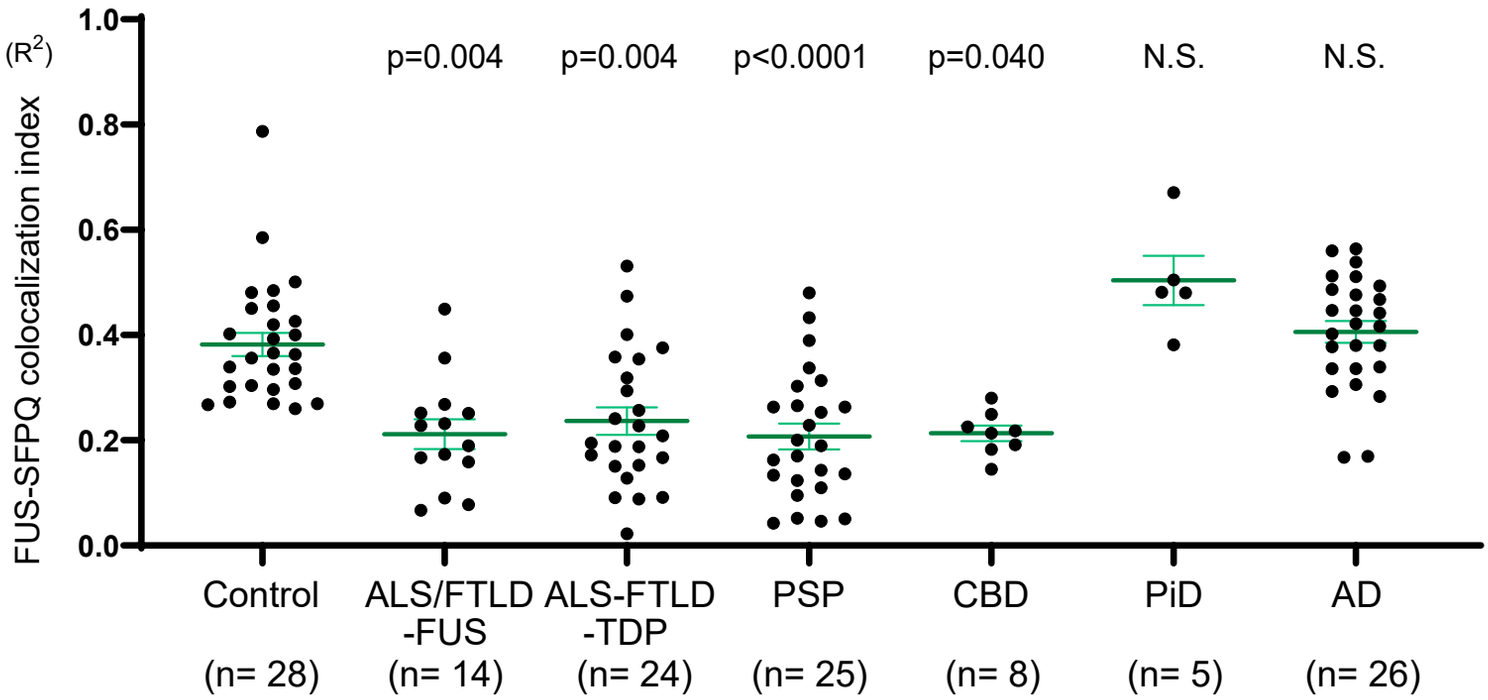
(R2)
FUS-SFPQ colocalization index
1.0
0.8
0.6
0.4
0.2
0.0
p=0.004
p=0.004
p<0.0001
p=0.040
N.S.
N.S.
Control
(n= 28)
ALS/FTLD -FUS
(n= 14)
ALS-FTLD -TDP
(n= 24)
PSP
(n= 25)
CBD
(n= 8)
PiD
(n= 5)
AD
(n= 26)

Figure 3

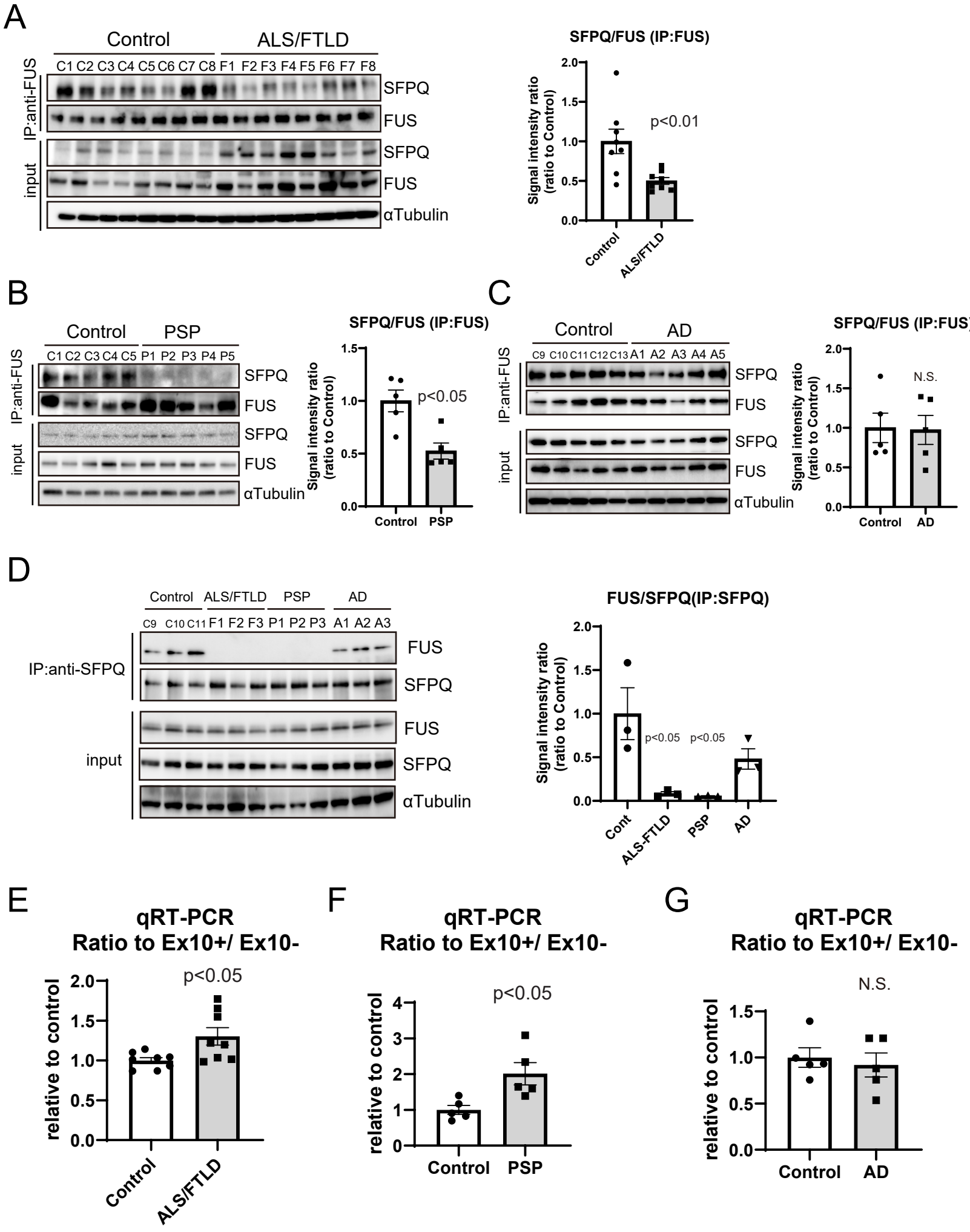
A
Control
ALS/FTLD
C1 C2 C3 C4 C5 C6 C7 C8 F1 F2 F3 F4 F5 F6 F7 F8
IP:anti-FUS
input
SFPQ
FUS
SFPQ
FUS
αTubulin
SFPQ/FUS (IP:FUS)
Signal intensity ratio (ratio to Control)
p<0.01
Control
ALS/FTLD
B
Control
PSP
C1 C2 C3 C4 C5 P1 P2 P3 P4 P5
IP:anti-FUS
input
SFPQ
FUS
SFPQ
FUS
αTubulin
SFPQ/FUS (IP:FUS)
Signal intensity ratio (ratio to Control)
p<0.05
Control
PSP
C
Control
AD
C9 C10 C11 C12 C13 A1 A2 A3 A4 A5
IP:anti-FUS
input
SFPQ
FUS
SFPQ
FUS
αTubulin
SFPQ/FUS (IP:FUS)
Signal intensity ratio (ratio to Control)
N.S.
Control
AD
D
Control
ALS/FTLD
PSP
AD
C9 C10 C11 F1 F2 F3 P1 P2 P3 A1 A2 A3
IP:anti-SFPQ
input
FUS
SFPQ
FUS
SFPQ
αTubulin
FUS/SFPQ(IP:SFPQ)
Signal intensity ratio (ratio to Control)
p<0.05
p<0.05
Cont
ALS-FTLD
PSP
AD
E
qRT-PCR
Ratio to Ex10+/ Ex10-
relative to control
p<0.05
Control
ALS/FTLD
F
qRT-PCR
Ratio to Ex10+/ Ex10-
relative to control
p<0.05
Control
PSP
G
qRT-PCR
Ratio to Ex10+/ Ex10-
relative to control
N.S.
Control
AD

Supplementary Information

Supplementary Figure 1: Quantification of FUS and SFPQ intranuclear colocalization

(A) We compared the immunostaining of different anti-FUS and anti-SFPQ antibody clones on a control brain sample using double immunofluorescence. A mouse-monoclonal anti-FUS antibody from Santa Cruz (4H11) was combined with a rabbit-polyclonal anti-FUS antibody from either Bethyl Laboratories (293A) or Sigma-Aldrich. Convergence of the fluorescent antibody signals within the nuclei of hippocampal granule cells was considered evidence for reliable immunolabeling of the FUS protein (data not shown). The immunostaining of two additional anti-SFPQ antibodies, a mouse-monoclonal antibody from Sigma-Aldrich and Abcam (B92), and a rabbit-polyclonal antibody from Bethyl Laboratories, were also compared. Signals from these two clones likewise indicated their sufficiency for use. Secondary fluorescent antibodies we used were conjugated Alexa-488 and 546 (1:1000, Thermo Fisher Scientific). (B) Hippocampal granule cells that were immunostained with anti-SFPQ, FUS, and NeuN antibodies and counter-stained with DAPI are shown at 40x magnification (left) and at 630x magnification (right). Fluorescent signals for intranuclear FUS and SFPQ were obtained at 630x magnification. Scale bars, 200 μm for left, 10 μm for right images. (C) Fluorescent signals for intranuclear FUS and SFPQ were obtained at 630x magnification. Wavelengths of 488 and 546 nm were set as the fluorescent unit, and signal intensities from each intranuclear matrix were automatically measured along the largest nucleus diameter by ZEN2012 software (left images in the upper image-graph sets). The middle graphs represent FUS (red) and SFPQ (green) signal intensities on the *y*-axis given for each pixel on the *x*-axis along the diameter of

the nucleus. As shown in the right panels, correlation indices (R^2) were high when the FUS and SFPQ signals were coincident with each pixel. In contrast, the R^2 values were low when the proteins were spatially dissociated in the nucleus. For instance, hippocampal granule cells in the control sample had FUS-SFPQ colocalization indices of 0.45, 0.51, 0.78, and 0.48, whereas neurons from the disease group had values of 0.11, 0.025, 0.0082, and 0.029 (lower panels). Scale bars, 5 μm.

Supplementary Figure 2: Immunofluorescent imaging of intranuclear FUS and SFPQ

Images for the cases depicted in Fig. 1A are shown in lower magnification. The sections were immunostained with anti-FUS and anti-SFPQ antibodies and counter-stained with DAPI-based (blue) nuclear staining. Scale bars = 10 μm for upper images, 20 μm for lower images.

Supplementary Figure 3: Comparison of FUS-SFPQ interactions between neurons with and without FUS-positive cytoplasmic inclusions.

Triple immunostaining was performed using anti-SFPQ (monoclonal-mouse, Sigma-Aldrich), anti-FUS (polyclonal rabbit, Bethyl Laboratories, A300-293A), and anti-FUS (polyclonal rabbit, Sigma-Aldrich) antibodies. (A) Three of the included ALS/FTLD-FUS cases (case #3, #4, and #5) had FUS-immunopositive cytoplasmic inclusions in the hippocampal granule cells. The interaction of FUS and SFPQ was similarly impaired in neurons with and without cytoplasmic inclusions. Arrows indicate FUS-positive cytoplasmic inclusions. Opal 4-Color Kit (Parkin Elmer) was used for triple immunofluorescent study. Scale bars = 5 μm. (B) Quantification data also revealed no

significant differences in FUS-SFPQ interactions between neurons with and without the cytoplasmic FUS-positive inclusions. Data shown are mean ± SEM.

Supplementary Figure 4: Comparison of FUS-SFPQ interactions between neurons with and without inclusions positive for phosphorylated-TDP-43 or phosphorylated-tau

(A) The FUS-SFPQ intranuclear colocalization was compared between neurons with and without phosphorylated TDP-43 (p-TDP-43) inclusions in a representative ALS/FTLD-TDP case (left images). A comparison between neurons with or without phosphorylated-tau (p-tau) inclusions was also undertaken in PSP and CBD cases (middle and right images). The interaction of FUS and SFPQ was similarly impaired in neurons with and without the cytoplasmic inclusions. Scale bars = 10 μm. Arrows indicate neurons harboring p-TDP-43 or p-tau inclusions. Scale bars = 5 μm. (B) Quantification data also revealed no significant differences in FUS-SFPQ interactions between neurons with and without cytoplasmic FUS-positive inclusions. Data shown are mean ± SEM.

Supplementary Figure 5: Interactions between FUS and SFPQ are disrupted in the brain tissue of ALS/FTLD and PSP cases

Frozen frontal lobe tissues, which contained the cortex and subcortical white matter, from autopsied brains were suspended in 3 ml of cold TNE buffer with protease inhibitors (Roche), and homogenized in a dounce tissue grinder with 15 strokes of a loose pestle. The homogenate was centrifuged at 3000 x g for 10 min to remove debris and was centrifuged again at 14000 x g for 12 min. The antibodies used in

immunoprecipitation and immunoblotting are listed in Supplementary Table 1. The band intensities were measured using Multi Gauge software (Fujifilm).

(A) The control immunoprecipitation experiment using anti-FUS (A300-293A) and rabbit IgG with two control samples (C1 and C2) is shown. (B) Tau protein profiles were shown by a fractionation assay using sarcosyl. Protein extracts from the cases in Fig. 3 were fractionated into TBS-soluble and sarcosyl-insoluble fractions. The TBS-soluble fractions were immunoblotted with anti-4R-tau (4R-T) and anti-3R-tau (3R-T) antibodies. (C) The ratio of signal intensities for 4R-T/3R-T in Supplementary Fig. 5A are shown. Although the 4R-T/3R-T ratio was not significantly altered, it trended towards 4R-T dominance in ALS/FTLD cases relative to controls (left graph, n = 8 for each, student t-test). In contrast, the 4R-T/3R-T ratio was significantly increased in PSP cases relative to controls (middle graph, n = 5 for each), whereas there was no difference in AD cases and controls (right graph, n = 5 for each, student t-test). Data shown are mean ± SEM. (D) The sarcosyl-insoluble fractions were immunoblotted with anti-total tau (Tau-5) and anti-phosphorylated tau (HT7) antibodies. Phosphorylated tau was present in sarcosyl-insoluble fractions from the PSP and AD samples but not from ALS/FTLD cases.

Supplementary Figure 6: Variability of FUS and SFPQ expression in the hippocampal granule cells

To evaluate the expression levels of FUS or SFPQ in the individual neuronal nuclei, the signal intensities of the two proteins were acquired from 400 nuclei in the hippocampal granule cell nuclei. Sample images were acquired and analyzed using a BZ-X700 microscope (Keyence). We determined the degree of correlation between the two proteins with a regression analysis to evaluate the proportion of FUS and SFPQ

expression in the hippocampal granule cells for each sample. We defined the R^2 correlation coefficient as an FUS-SFPQ expression variability value. When the values are large, the expression of FUS and SFPQ in individual neurons is less variable. The FUS-SFPQ expression variability values were plotted and compared among the disease states.

(A) Anti-SFPQ and anti-FUS immunofluorescence images of hippocampal granule cells from representative cases are shown. The SFPQ (green) and FUS (red) signals were equivalent in a control sample but exhibited a variable mosaic expression pattern in cases with ALS-FUS, FTLD-TDP, PSP, and CBD. Scale bars, 10 μm. (B) Schematic diagram depicting our method for quantitatively determining the degree of FUS-SFPQ expression variability in representative cases. The left box denotes a control case, whereas the right box is for an ALS/FTLD-FUS case. Wavelengths at 488 and 546 nm were set as the fluorescent unit, and fluorescent signals were automatically acquired from the individual hippocampal granule cells using ZEN2012 software. After plotting the FUS and SFPQ signals for each hippocampal granule cell, a correlation index (R^2) was calculated. In the neurons of a control, the proportion of FUS and SFPQ was equivalent hence well correlated with a correlation index of 0.474. In a case with FTLD-FUS, the expressions of FUS and SFPQ were disproportional with a correlation index of 0.006. Scale bars, 10 μm. (C) In controls, the average FUS-SFPQ expression variability value was 0.20 ± 0.18. By contrast, the values were significantly lower in the cases with ALS/FTLD-FUS (0.053 ± 0.013, $p = 0.038$), ALS/FTLD-TDP (0.043 ± 0.008, $p < 0.0001$), and PSP (0.071 ± 0.158, $p = 0.003$) than that of controls (0.14 ± 0.12). The cases with AD (0.14 ± 0.12), CBD (0.070 ± 0.029), and PiD (0.13 ± 0.05) did not show significant differences when compared with the control. Kruskal-Wallis test was under

taken. Significance level was set at $p < 0.05$ after Bonferroni/Dunn correction of the raw p-values for seven group comparisons: the control (n = 28) vs. ALS/FTLD-FUS (n = 14), ALS/FTLD-TDP (n = 24), PSP (n = 25), CBD (n = 8), PiD (n = 5), or AD (n = 26). Data shown are mean ± SEM. (D) Scatter plots for all included individuals showed a significant correlation between the FUS-SFPQ expression variability indices and the FUS-SFPQ colocalization indices (linear least square method, $R^2 = 0.128$, $p < 0.001$).

Supplementary Table 1

Antibodies used in the study.

Figure	primary antibody	vender	#clone or product	source	experiment	dilution
Figure 1	anti-FUS	Bethyl Laboratories	A300-293A	rabbit-IgG	IF	1:1000
	anti-SFPQ	Sigma-Aldrich	WH0006421M2	mouse-IgG	IF	1:300
Figure 3	anti-FUS	Bethyl Laboratories	A300-293A	rabbit-IgG	IP	5 μg/ mg lysate
	anti-SFPQ	abcam	B92	mouse-IgG	WB	1:1000
	anti-FUS	Santa Cruz	4H11	mouse-IgG	WB	1:500
	anti-SFPQ	Bethyl Laboratories	A301-321A	rabbit-IgG	IP	5 μg/ mg lysate
	anti-αTubulin	Santa Cruz	10D8	mouse-IgG	WB	1:500
Supplementary Figure 1	anti-FUS	Bethyl Laboratories	A300-293A	rabbit-IgG	IF	1:1000
	anti-FUS	Santa Cruz	4H11	mouse-IgG	IF	1:300
	anti-FUS	Sigma-Aldrich	HPA008784	rabbit-IgG	IF	1:200
	anti-SFPQ	Sigma-Aldrich	WH0006421M2	mouse-IgG	IF	1:300
	anti-SFPQ	Bethyl Laboratories	A301-321A	rabbit-IgG	IF	1:1000
	anti-NeuN	abcam	EPR12763	rabbit-IgG	IF	1:1000
Supplementary Figure 2	anti-FUS	Bethyl Laboratories	A300-293A	rabbit-IgG	IF	1:1000
	anti-SFPQ	Sigma-Aldrich	WH0006421M2	mouse-IgG	IF	1:300
Supplementary Figure 3	anti-FUS	Bethyl Laboratories	A300-293A	rabbit-IgG	IF	1:1000
	anti-SFPQ	Sigma-Aldrich	WH0006421M2	mouse-IgG	IF	1:300
	anti-FUS	Sigma-Aldrich	HPA008784	rabbit-IgG	IHC	1:200

Supplementary Figure 4	anti-FUS	Bethyl Laboratories	A300-293A	rabbit-IgG	IF	1:1000
	anti-SFPQ	Sigma-Aldrich	WH0006421M2	mouse-IgG	IF	1:300
	anti-phosphorylated TDP-43	Cosmo Bio	S409/410	rabbit-IgG	IF	1:1000
	anti-phosphorylated tau	Thermo Fisher	AT8	mouse-IgG	IF	1:200
Supplementary Figure 5	anti-3R-T	Millipore	RD3	mouse-IgG	WB	1:2000
	anti-4R-T	Millipore	RD4	mouse-IgG	WB	1:1000
	anti-phosphorylated tau	Thermo Fisher	HT7	mouse-IgG	WB	1:1000
	anti-total-tau	abcam	TAU-5	mouse-IgG	WB	1:2500
Supplementary Figure 6	anti-FUS	Bethyl Laboratories	A300-293A	rabbit-IgG	IF	1:1000
	anti-SFPQ	Sigma-Aldrich	WH0006421M2	mouse-IgG	IF	1:300
Pathological validation	anti-TDP-43	Proteintech	10782-2-AP	rabbit-IgG	IHC	1:200
	anti-phosphorylated TDP-43	Cosmo Bio	S409/410	rabbit-IgG	IHC	1:1000
	anti-phosphorylated tau	Thermo Fisher	AT8	mouse-IgG	IHC	1:200
	anti-β-amyloid	Dako	6F3D	mouse-IgG	IHC	1:300
	anti-FUS	Bethyl Laboratories	A300-293A	rabbit-IgG	IHC	1:1000
	anti-FUS	Sigma-Aldrich	HPA008784	rabbit-IgG	IHC	1:200
	anti-SFPQ	Sigma-Aldrich	WH0006421M2	mouse-IgG	IHC	1:300

Supplementary Table 2

Primers used for qPCR.

Gene	Forward	Reverse	Internal probe
human MAPT exon10- (3R-T)	ACCTGAAGAATGTCAAGTC	GATGGATGTTGCCTAATGA	AGACTATTTGCACCTTCCCGCCTC
human MAPT exon10+ (4R-T)	GTGCAGATAATTAATAAGAAGC	GATGGATGTTGCCTAATG	

Supplementary Figure 1

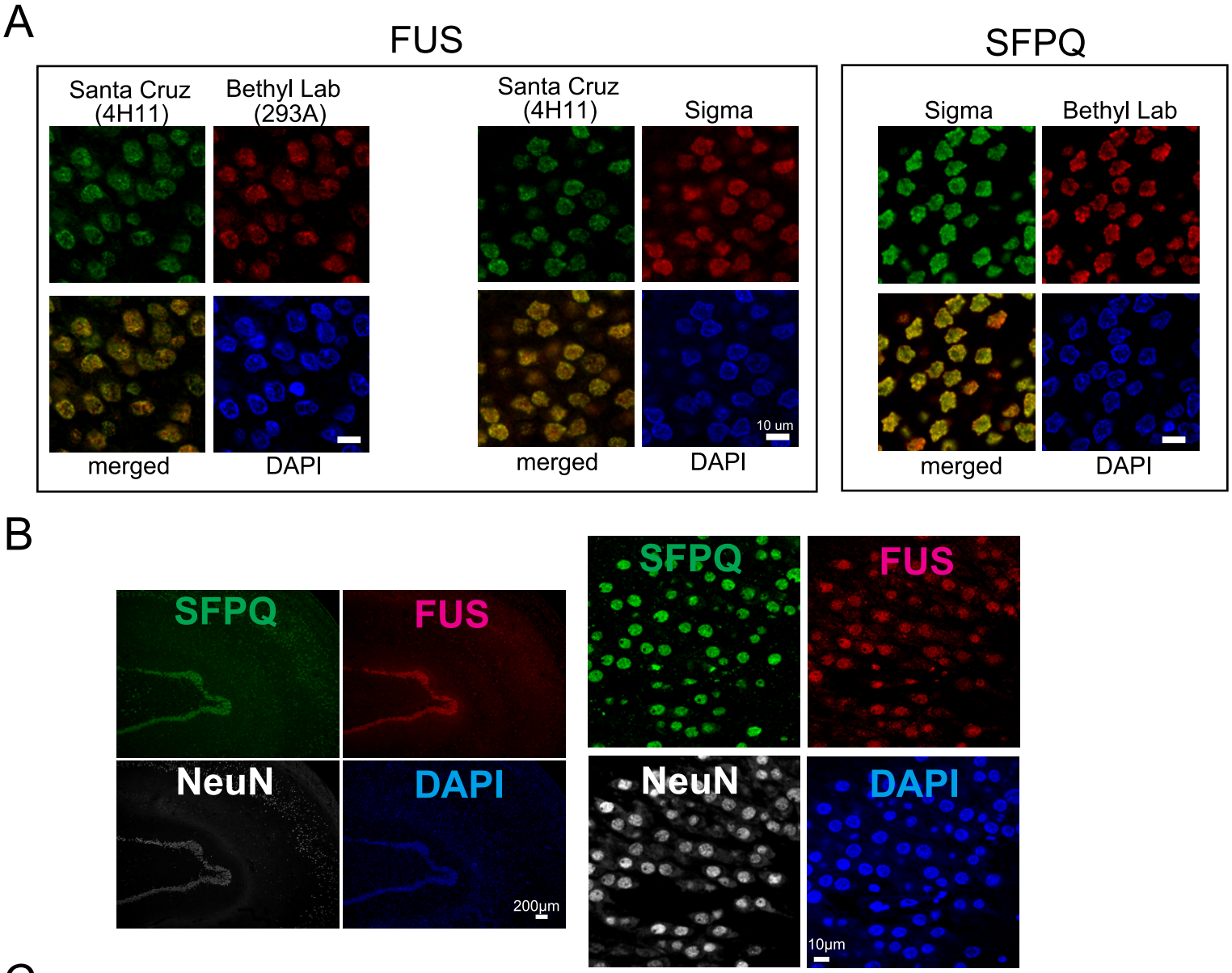

Supplementary Figure 2

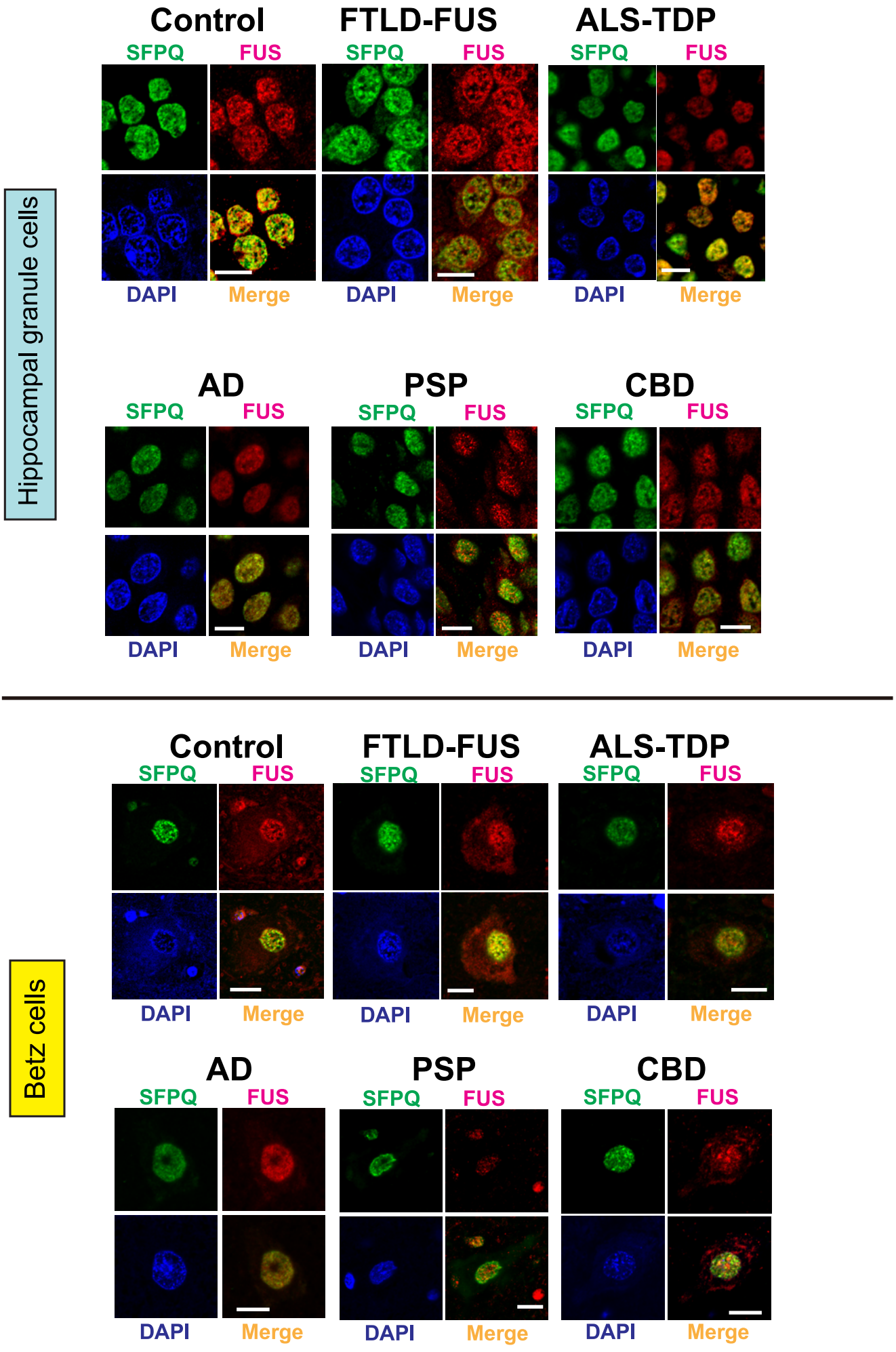

Supplementary Figure 3

A

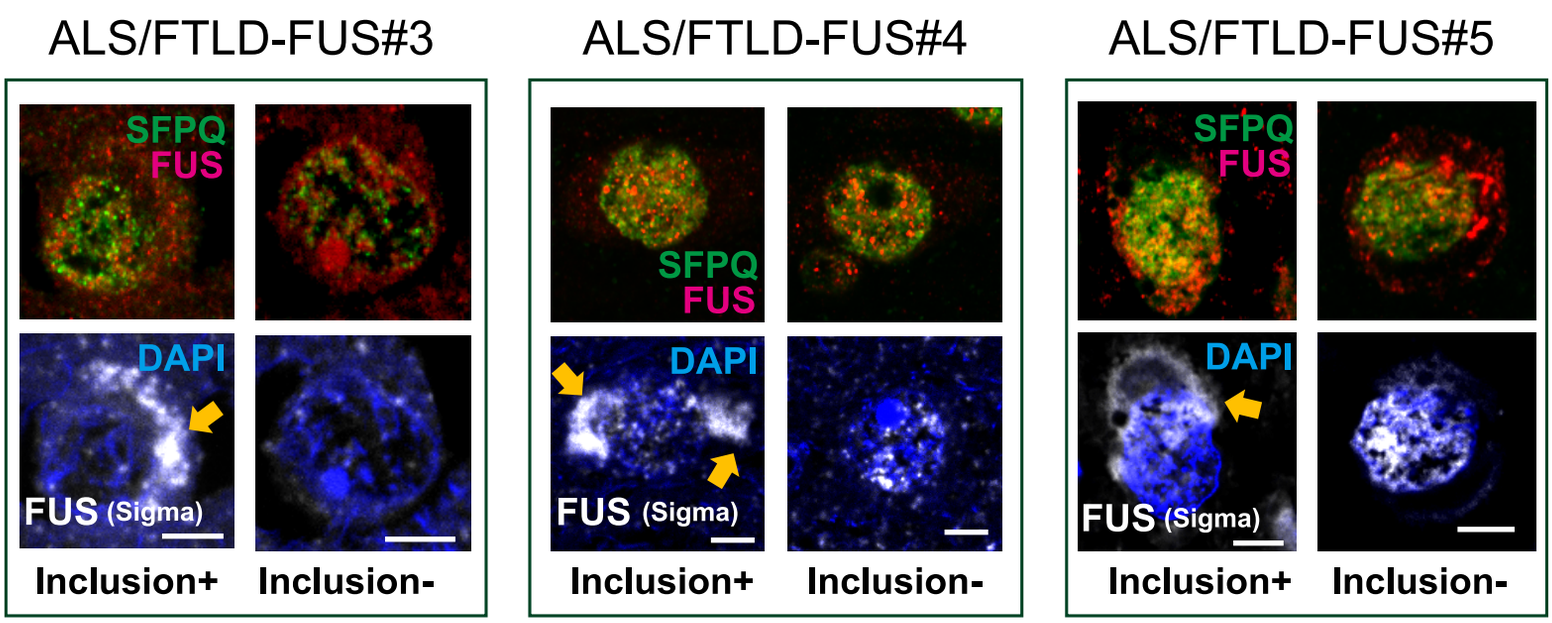

B

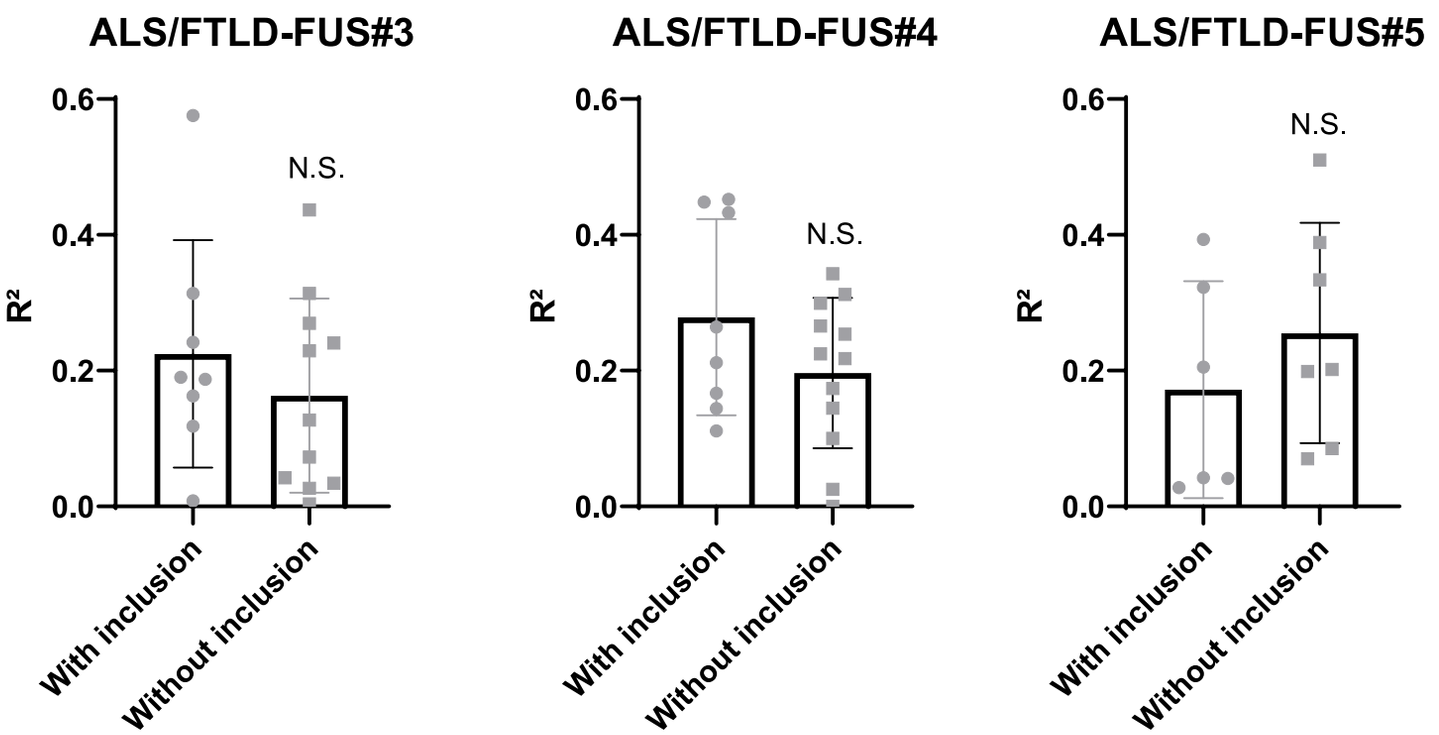

Supplementary Figure 4

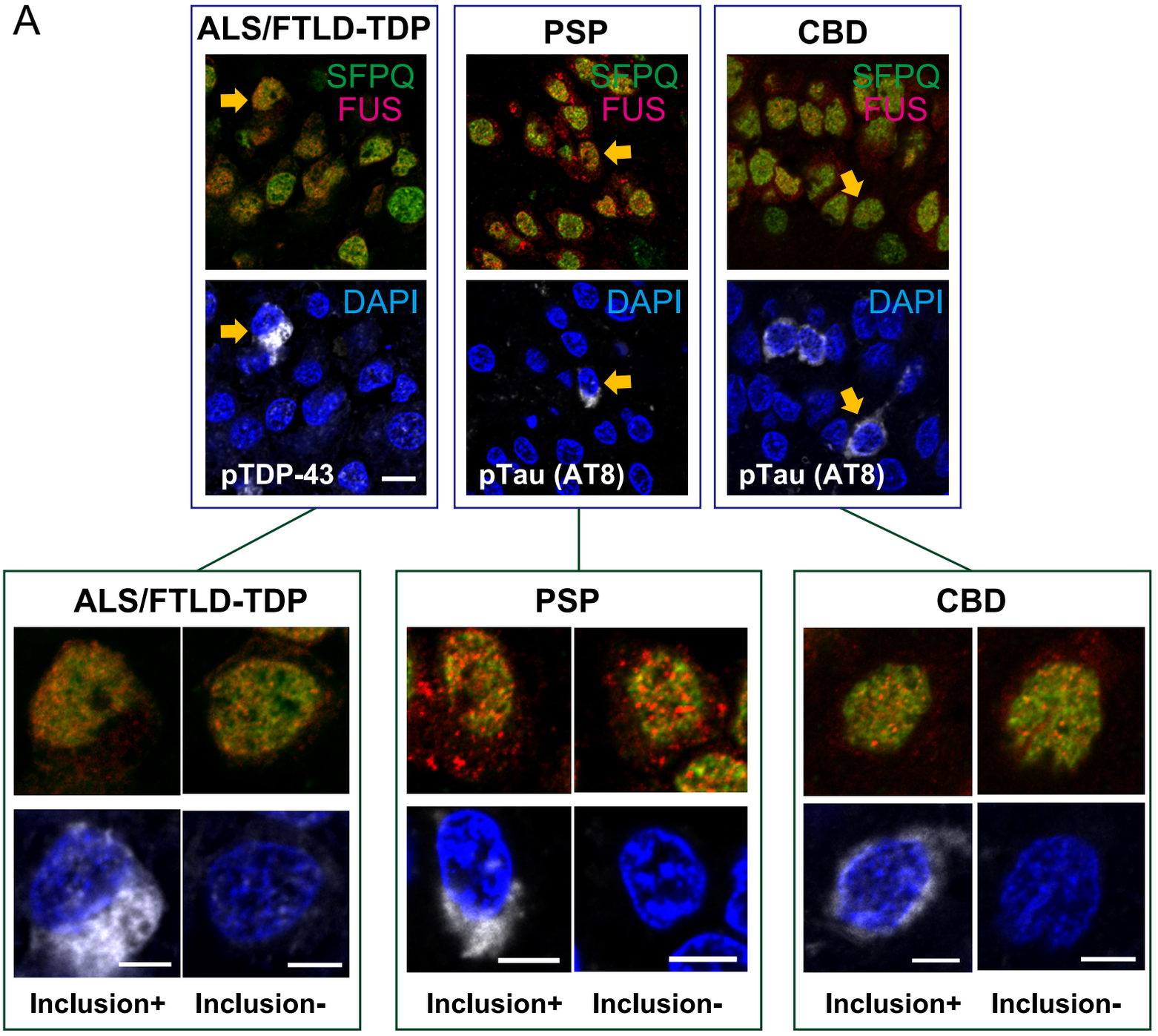

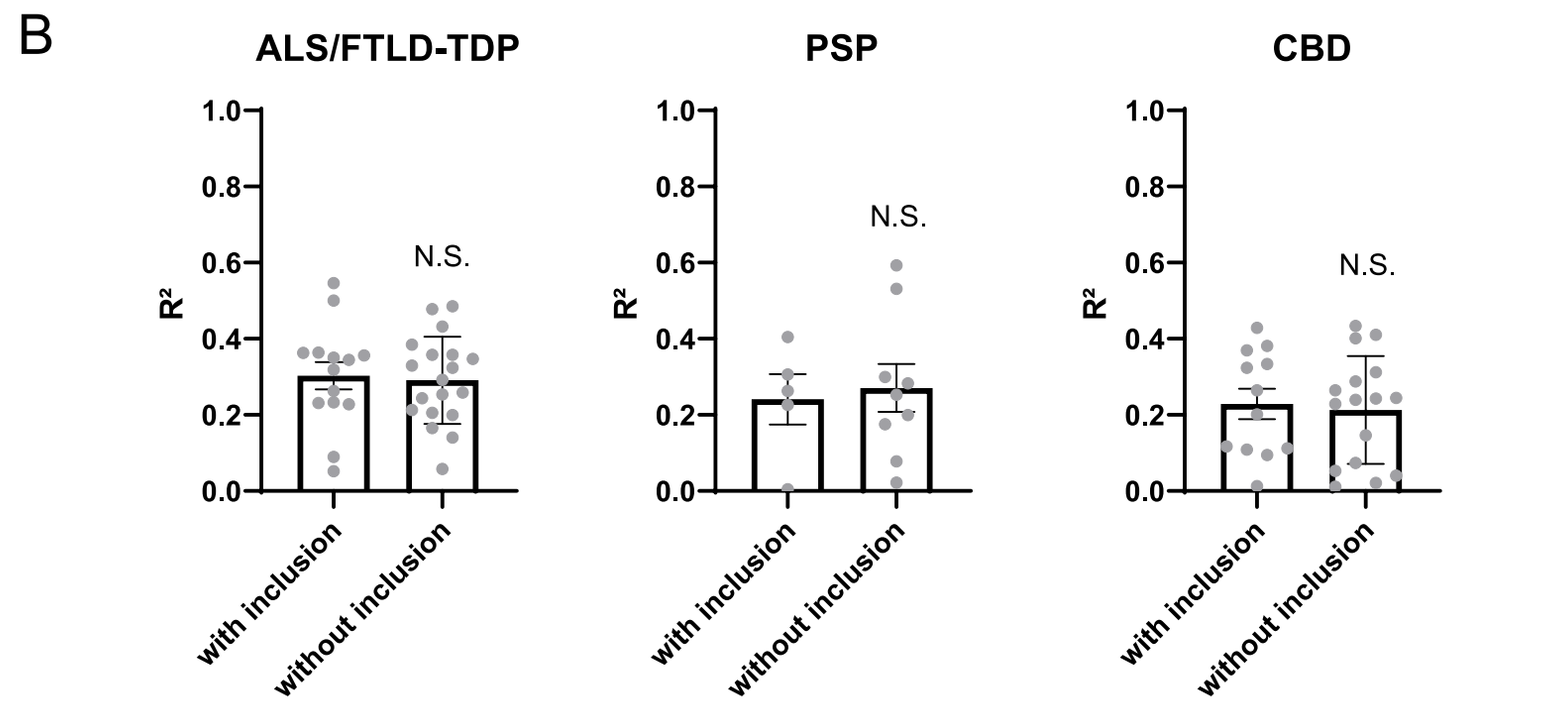

Supplementary Figure 5

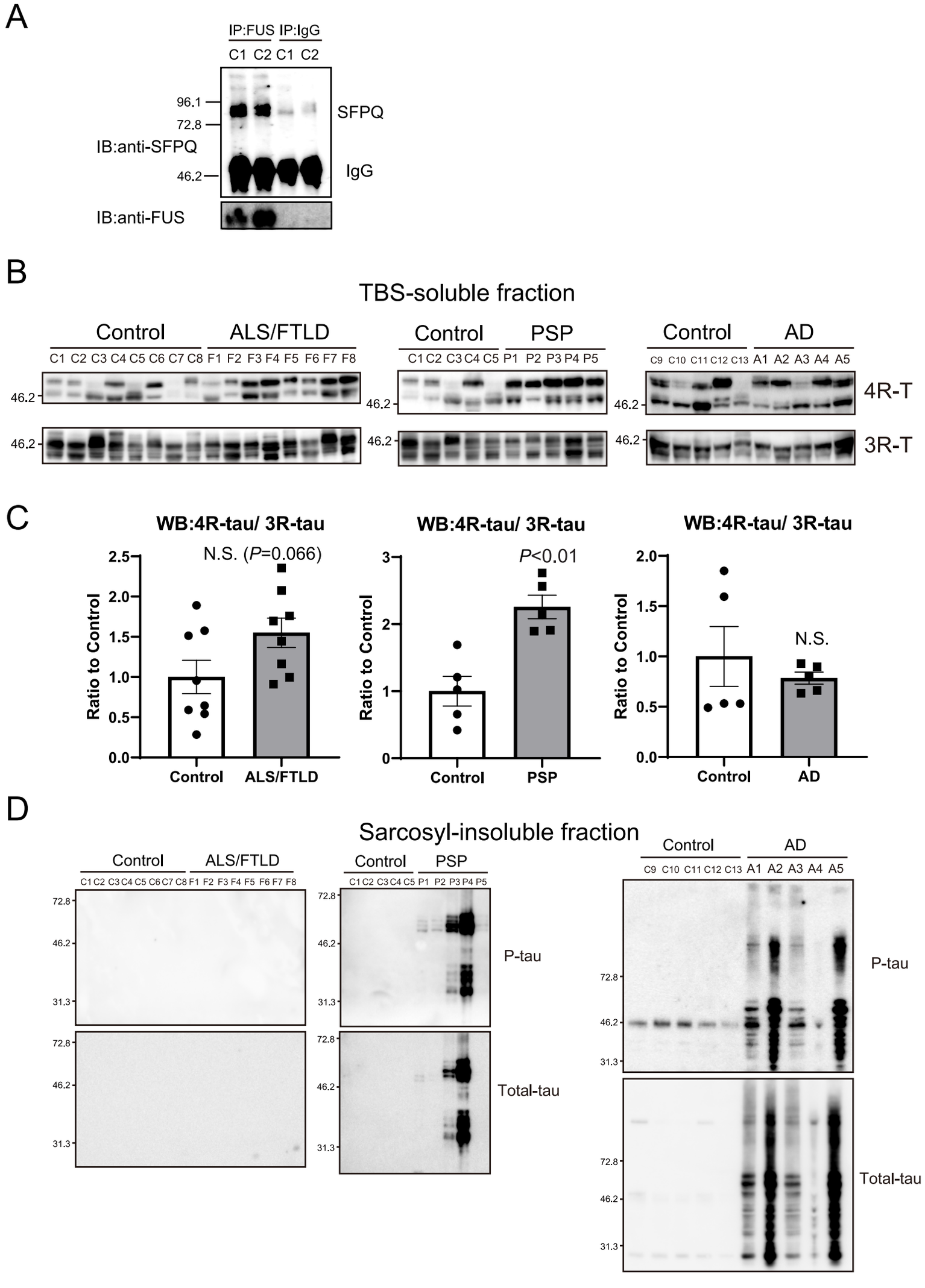

Supplementary Figure 6